Generation of Photon Pairs in Dispersion Shift Fibers through Spontaneous Four Wave Mixing: Influence of Self-phase Modulation

Xiaoxin Ma, Lei Yang, Xueshi Guo, Xiaoying Li*

College of Precision Instrument and Opto-electronics Engineering, Tianjin University, Key Laboratory of Optoelectronics Information Science and Technology, Ministry of Education, Tianjin, 300072, P. R. China

Abstract

Correlated signal and idler photon pairs with small detuning in the telecom band can be generated through spontaneous four-wave mixing in dispersion shift fibers. However, photons originated from other nonlinear processes in optical fibers, such as Raman scattering and self-phase modulation, may contaminate the photon pairs. It has been proved that photons produced by Raman scattering are the background noise of photon pairs. Here we show that photons induced by self-phase modulation of pump pulses are another origin of background noise. After studying the dependence of self-phase modulation induced photons in signal and idler bands, we demonstrate that the quantum correlation of photon pairs can be degraded by the self-phase modulation effect. The investigations are useful for characterizing and optimizing an all fiber source of photon pairs.

Keywords: photon pairs, fiber, spontaneous four wave mixing, self-phase

*Corresponding author. Tel.: +86-22-27406476
Email address: xiaoyingli@tju.edu.cn (Xiaoying Li)

modulation

Quantum correlated photon pairs are not only the important resources for fundamental test of quantum physics, but also crucial for quantum metrology and quantum information processing. Recently, there has been growing interest in generating photon pairs by means of spontaneous four-wave mixing (SFWM) in single mode optical fibers, owing to the advantage of single spatial mode and the potential to develop into a practical quantum device. So far, photon pairs with different kinds of wavelengths and spectra have been realized by using various kinds of optical fibers, including dispersion shift fibers (DSFs), high nonlinear optical fibers, and photonic crystal fibers [1–5]. Moreover, based on these photon pairs, heralded single photon sources and entangled photon pairs with different degrees of freedom have been realized [6–10].

It is worth noting that among the various kinds of photon pairs, photon pairs in the 1550 and 1310 nm bands produced via SFWM in DSFs and standard optical fibers, respectively, are promising candidates for an all-fiber source having the advantages of compact size and freedom from misalignment [1, 11], since off-the-shelf fiber components with high quality and low cost are commercially available in the telecom bands. Moreover, for the fiber source of photon pairs in telecom bands, which are compatible with optical network and highly desirable for long distance quantum communication, the phase-matching conditions of SFWM are satisfied when the central wavelength of pump is in the anomalous dispersion regime, and the detunings of non-degenerate signal and idler photon pairs are usually small. Under this condition, photons having the same frequency as the individual signal or

idler photons may also produced by other nonlinear processes, such as Raman scattering (RS) and self-phase modulation (SPM) of the pump pulses. It has been proved that photons produced by RS are the background noise of photon pairs. To improve the quality of the sources of photon pairs, a lot of efforts have been made on characterizing and minimizing the effect of RS, such as reducing the detuning of photon pairs, decreasing the duration of pump pulses, and lowering the temperature of optical fibers etc. [2, 12–15]. The influence of SPM induced photons, on the other hand, has not been fully characterized, although there are a few experimental reports showing that SPM might become the dominate origin of scattered photons when the detuning is reduced [13, 16].

In this paper, using 300-meter-long DSF pumped by a pulsed pump with the central wavelength in the anomalous dispersion regime, we experimentally study how the SPM of pump affect the quality of the source of photon pairs in 1550 nm band. After properly separating the SPM induced photons from those originated from SFWM and RS, we characterize its dependence upon the detuning of photon pairs, and upon the power and bandwidth of pump pulses. Moreover, we experimentally demonstrate that quantum correlation of photon pairs can be degraded by the SPM induced noise photons. Our investigations is not only helpful for developing an all fiber source of photon pairs with low background noise, but also useful for exploring its applications [17, 18].

Our experimental setup, which is similar to that in Ref.[16], is shown in Fig. 1. A piece of 300 m DSF, with the zero dispersion wavelength of $\lambda_0 = 1537 \pm 2\,\mathrm{nm}$ is submerged in liquid nitrogen (77 K) to suppress RS. The

fiber polarization controller (FPC_1) is used to compensate the birefringence introduced by bending and coiling of the DSF. When the pump pulses with a central wavelength of 1538 nm are launched into the DSF, the parametric process of SFWM is phase-matched and the probability of the four photon scattering is significantly enhanced. In this process, two pump photons at frequency ω_p scatter through the Kerr ($\chi^{(3)}$) nonlinearity of the fiber to create energy-time entangled signal and idler photons at frequencies ω_s and ω_i, respectively, such that $2\omega_p = \omega_s + \omega_i$. Meanwhile, accompanying SFWM, photons at frequencies ω_s and ω_i are also produced by RS and SPM of pump pulses.

The photons scattered from different nonlinear processes have their own characteristics. For SFWM, signal and idler photons are created in pair-wise and predominately co-polarized with pump, the sum of the phases of the twin photons equals to that of the two pump photons, but the phase of individual signal and idler photon is random; for RS, a signal or idler photon, originated from a pump photon scatters off an optical phonon, randomly takes the polarization and phase; while for SPM, signal and idler photons come from spectral broadening of pump pulses, will inherit the polarization and phase information of the pump photons. If we only think of the individual signal or idler photons, those via SFWM and RS are in thermal state, while those originated from SPM are in coherent state.

To study the influence of SPM on the quantum correlation of photon pairs, it is necessary to separate the SPM induced photons from those originated from SFWM and RS. To achieve this, before launching into the DSF, pulsed pump are decomposed into horizontally and vertically polarized components,

P_H and P_V, respectively, by use of a polarization beam splitter PBS_1 (see Fig. 1). P_H and P_V, which propagate in clockwise and counter clockwise directions, respectively, with relative phase difference of ϕ, will independently produce signal and idler photons via $\chi^{(3)}$ nonlinearity. At the output port of PBS_1, apart from the residual pump photons, there are three kinds of photons at frequencies ω_s and ω_i emerged: (i) co-polarized signal and idler photons created in pair-wise via SFWM; (ii) co-polarized signal and idler photons via RS; and (iii) signal and idler photons originated from SPM. For the individual signal or idler photons produced by SPM of P_H and P_V, respectively, the ideal first order interference is observable. Whereas the signal or idler photons produced by SFWM of P_H and P_V, respectively, are equivalent to two independent thermal fields, it is impossible to observe the first order interference between them. So do the photons via RS.

To form the first order interference to sort out SPM induced photons, the polarization of signal and idler photons emerged at the output port of PBS_1 are rotated 45 degree respect to its original horizontal and vertical directions by adjusting FPC_2. Then, the photons propagate through PBS_2 and filter F. The filter F has the function of well separating signal, idler, and pump photons, and the central wavelengthes of the detected signal and idler photons with a FWHM of about 0.65 nm can be varied by adjusting F, which is realized by cascading a free-space double-grating spectral filter with tunable filters [16]. Since the Kerr nonlinearity is weak, only about 0.1 photon pairs are typically produced by a 5 ps pump pulse containing 5×10^7 photons, to reliably detect the photon pairs, the pump-rejection ratio provided by F should be greater than 100 dB. When the signal and

idler photons are detected by using single photon detectors SPD_3 and SPD_2, respectively, and the powers of P_H and P_V are equal, the measured counting rate of $SPD_{2(3)}$ can be expressed as:

$$N_t = N_F + N_R + N_S\,(1 + \cos\phi) \tag{1}$$

where N_F, N_R and N_S are count rate of photons produced from SFWM, RS and SPM, respectively. By scanning the relative phase ϕ between P_H and P_V, a cosine variation can be obtained, from which N_S can be extracted. Since the counting rate of SPM induced photons in signal band is slightly smaller than that in idler band due to asymmetry in spectrum broadening of the pump, for the counting measurement of individual signal or idler photons, we only present the results of idler photons for convenience.

The function of scanning the relative phase difference ϕ is realized by decompounding the linearly polarized pump in the port labelled "pump in" and adding separate free-space propagation paths for the two decomposed pumps, P_H and P_V, with use of the PBS_3, quarter-wave plates QWP_1 and QWP_2, and mirrors M_1 and M_2 (see Fig. 1). This arrangement is equivalent to a polarization interferometer formed between PBS_3 and PBS_2. The linearly polarized pump with a Gaussian shaped spectrum is obtained by using a filter to spectrally carve the output of a mode-locked femto-second fiber laser having a repetition rate of about 41 MHz [18], and the time bandwidth product of pump is about 0.6. M_2 is mounted on a piezoelectric-transducer (PZT)-driven translation stage, which allows precise adjustment of the relative delay and phase difference between P_H and P_V. In our experiment, the relative delay is adjusted to be 0. To monitor the phase difference ϕ, the residual pump photons, separated by the filter F, are attenuated to sin-

gle photon level and then measured by using SPD_1. The power of P_H is adjusted to be equal to that of P_V by properly regulating half-wave plate HWP_1. Therefore, the counting rate of SPD_1, n_p, can be expressed as

$$n_p \propto N_p \left(1 + \cos\phi\right), \tag{2}$$

where N_p is determined by the intensity of P_H (P_V).

The SPDs used for conducting the photon counting measurement are InGaAs/InP avalanche photodiode based SPDs (PLI-AGD-SC-Rx and id200) operated in the gated-Geiger mode. The 2.5-ns-wide gate pulses arrive at a rate of 1.29 MHz, which is 1/32 of the repetition rate of the pump pulses, and the dead time of the gate is set to be 10 μs. The timing of gate pulses is adjusted by a digital delay generator to coincide with the arrival of idler, signal, or attenuated pump photons. The electrical signals produced by the SPDs in response to the incoming photons (and dark events), reshaped into 100-ns wide TTL pulses, are then acquired by a computer-controlled analog-to-digital (A/D) board (National Instrument, PCI-6251). Thus, both the single counts of each SPD and two-fold coincidences of SPD_2 and SPD_3 acquired from different time bins can be determined because the A/D card records all counting events. The total detection efficiency of the idler (signal) photons is about 2%.

Before characterizing the SPM induced photons in idler band, we first find out the possible smallest value of detuning between idler (signal) and pump photons, $\Omega = (\omega_{i(s)} - \omega_p)/2\pi$, at which the signal and idler photons contained in the incident pump pulses, P_H and P_V, are negligible, and pump-rejection ratio provided by filter F in signal and idler bands is greater than 100 dB. In the measurement, the FWHM of the Gaussian shaped pump pulses is about

0.95 nm, and the DSF is taken away. The photon counting measurements in idler band are conducted when the detuning Ω is varied with a step of 50 GHz (0.4 nm). Meanwhile, to monitor the phase difference ϕ, the counting rate of the attenuated pump photons n_p is also recorded. At each detuning, we record the single counts of SPD_1 and SPD_2, respectively, as the relative phase difference ϕ is scanned. Figure 2(a) plots the measured counting rates as a function of ϕ when the average pump powers of both P_H and P_V are 0.1 mW ($\sim 2 \times 10^7$ photons/pulse). It is clear that the count rate presents periodic variation at the detuning $\Omega = 0.4$ THz (3.2 nm), showing there are photons detected in idler (and signal) band even if nonlinear medium DSF is absent; whereas the periodic variation is not obvious when Ω is greater than 0.45 THz (3.6 nm). Taking the total detection efficiency in idler band into account, we are able to deduce that the ratio between the number of photons in idler and in pump bands per pulse is about 2.5×10^{-10} and 2.5×10^{-11} for $\Omega = 0.4$ THz and $\Omega = 0.45$ THz, respectively. Therefore, the pump-rejection ratio of filter F is more than 100 dB for Ω greater than 0.45 THz (3.6 nm), namely, the possible smallest detuning is about 3.6 nm.

Considering the spectra of pumps, P_H and P_V, might be broadened in DSF due to SPM, we start to characterize the SPM induced photons at the detuning of 4 nm, which is slightly greater than the smallest detuning deduced from the above measurement. In this measurement, we put the DSF back and make the same measurement again when the average powers for both P_H and P_V are about 90 μW. Figure 2(b) shows the counting rates recorded by SPD_1 and SPD_2, respectively, as a function the relative phase difference ϕ. Fitting the data with Eqs. (1) and (2), we find that the peri-

odicity of the count rate in idler band is the same as that of the pump, and the extracted rate N_S, proportional to the SPM induced photons, is about 70% of the total counting rate $N_t' = N_F + N_R + N_S$. Therefore, the photons originated from SPM effect could almost dominate over SFWM even if the filter F can provide a pump isolation in excess of 100 dB.

To figure out the power dependence of N_S, we further increase the detuning to 4.4 nm, and repeat the above measurement at different power levels of P_H (P_V). At each power level, after extracting the the counting rate N_S from the measured results of N_t, we fit the counting rate of the photons originated from RS and SFWM and, $N_R + N_F$, with the second-order polynomial $s_1 P_{ave} + s_2 P_{ave}^2$, where the linear and quadratic coefficients, s_1 and s_2, respectively determine the strengths of RS and SFWM in DSF, and P_{ave} refers to the average power of P_H (P_V). The main plot in Fig. 3 shows the counting rates N_S and $N_F + N_R$, respectively, as a function of the average power of pump P_H (P_V). The inset of Fig. 3 sketches the ratio N_S/N_F versus the average power of P_H (P_V). One sees that N_S exponentially increases with the increase of pump power. Additionally, although N_S is small at low pump power levels, it is still comparable with the photon counting rate N_R originated RS.

The experimental results in Fig. 2 and Fig. 3 indicate that without carefully excluding the noise photons coming from SPM, it would be impossible to precisely characterize the photon pairs produced by SFWM. Therefore, it is necessary to further investigate the factors influencing the counting rate N_S. Firstly, we study the influence of detuning at different pump powers. The measurement process is similar to previous, except the detuning is ad-

justed from 4.4 to 6 nm. At each detuning, we deduce the ratio N_S/N_F when the power level of P_H (P_V) is 140, 190 and 240 μW, respectively, as shown in Fig. 4. One sees that at a certain pump power, N_S/N_F decreases rapidly with the increase of detuning; while at a certain detuning, N_S/N_F increases with the increase of pump power. For the power level of $P_H = P_V = 190$ μW, N_S/N_F is less than 5% when detuning is greater than 4.8 nm; while for the power level of $P_H = P_V = 240$ μW, to obtain the ratio N_S/N_F less than 5%, the detuning should be greater than 5.2 nm. The result indicates that in order to suppress the SPM effect, the higher the power of pump, the greater the detuning is required.

Secondly, we study the influence of the bandwidth of pump. After modifying the FWHM of the pump to 0.65 nm, we make the photon counting measurement again by varying the detuning from 4 to 4.8 nm for the pumps with power level of $P_H = P_V = 240$ μW. The results are also plot in Fig. 4. One sees that for the same detuning, the ratio N_S/N_F obtained by using the pump with FWHM of 0.65 nm is the smallest. Moreover, if we consider that the counting rate of photons via SFWM, N_F, obtained by using this pump is higher than that obtained by using the pump with FWHM and power of 0.95 nm and 140 μW [18], respectively, it is then obvious that the negative effect of SPM to the fiber source of photon pairs decreases with the reduction of the bandwidth of pump.

In fact, the experimental results displayed from Fig. 2 to Fig. 4 can be qualitatively explained by using a simplified theoretical model. Assuming the strong pumps launching into DSF are transform limited, the Fourier

transform of the pulses propagating through the DSF is given by

$$E(z,\omega) \propto \int \sqrt{P_p}\exp(-\frac{T^2}{2T_0^2})\exp[i\gamma P_p z e^{-T^2/T_0^2}]\exp[i(\omega-\omega_{p0})T]dT. \quad (3)$$

where P_p and ω_{p0} are the peak power and the central frequency of pump, respectively; γ is the nonlinear interaction coefficient. In this case, the number of photons in the original pump pulse can be expressed as

$$N_p = \frac{1}{2\pi\hbar\omega_{p0}}\int_{-\infty}^{\infty}|E(0,\omega)|^2\,d\omega, \quad (4)$$

and the number of the SPM induced photons in idler/signal band can be written as

$$N_{Si(s)} = \frac{1}{2\pi\hbar\omega_{i(s)0}}\int_{-\infty}^{\infty}|E(L,\omega)|^2\,f_{i(s)}(\omega)d\omega, \quad (5)$$

where L is the length of DSF, $f_{i(s)}(\omega)$ and $\omega_{i(s)0}$ are the transmission function and central frequency of the filter in idler (signal) band, respectively.

Because the detuning of photon pairs produced via SFWM in DSF is small, to ensure a reliable detection of photon pairs, we need to take the rejection of the pump photons with spectrum broadened by SPM into account. Therefore, for the filter F in signal and idler band, not only a greater than 100 dB isolation to the original pump photons is necessary, the condition

$$N_{Si(s)}/N_p < 10^{-10} \quad (6)$$

is also required. Assuming the group velocity dispersion effect can be neglected, at the output port of the DSF, the spectral broadening factor of the pump pulse is about $\sqrt{1+(0.88\gamma P_p L)^2}$ [19]. In this case, for the filter in idler (signal) band described by a Gaussian function, the minimum detuning satisfying Eq. (6) is approximately:

$$\left|\lambda_{i(s)0}-\lambda_{p0}\right| > \sqrt{10\ln 10}\sqrt{\sigma_p^2[1+(0.88\gamma P_p L)^2]+\sigma_{i(s)}^2} \quad (7)$$

where $\lambda_{p(i,s)0}$ is the central wavelength of the pump (idler, signal) photons; $\sigma_p = \lambda_{p0}^2/(2\pi c T_0)$ is 1/e half-width of input pump, and $\sigma_{i(s)}$ is 1/e half-width of filter in idler (signal) band. According to Eq. (7) we plot the relationship between the minimum detuning and average pump power for the pump with FWHM of 0.95nm and 0.65nm, respectively. It is clear that the tendency shown in Fig. 5 agrees with our experimental data, except the calculated minimum detuning is smaller than that in our experiments. We think the main reason accounting for this departure is: the pump pulses are also influenced by chromatic dispersion, so the spectrum broadening is more severe. If the chromatic dispersion parameters of the DSF can be accurately measured, it would be possible to obtain a rigorous result of power distribution of the broadened pump in the spectral domain by using time-domain Schindinger equation [19].

Having investigated the dependence of N_S, we finally demonstrate that photon pairs via SFWM can be contaminated by the SPM induced photons. In this experiment, we rotate HWP_1 to ensure only the vertically polarized pump P_V is launched into DSF ($P_H = 0$), and adjust FPC_2 to select the co-polarized signal and idler photons (see Fig. 1). During the measurement, the FWHM of pump is about 0.95 nm, the coincidence and accidental coincidence rate of signal and idler photons C_c and C_a, produced by the same pulse and adjacent pulses, respectively, are recorded at different power levels. To show the influence of SPM, the measurement is conducted for the detunings of 4.4 and 5.6 nm, respectively. Moreover, for each measurement, we calculate the true coincidence by subtracting C_a from C_c, which is a reflection of the quantum correlation of photon pairs. The main plot in Fig. 6 shows the true-

coincidence to accidental-coincidence ratio (TAR) $R_T = \frac{C_c - C_a}{C_a}$ as a function of pump powers. One sees that when the pump power is lower than 0.15 mW, TAR obtained with detuning of 4.4 nm is slightly higher. However, when the pump power is higher than 0.2 mW, TAR obtained with detuning of 4.4 nm is obviously smaller, and the difference of TAR obtained under the two kinds of detunings increases with the increase of pump.

The results in the main plot of Fig.6 can be understood by analyzing the dependence of TAR R_T. At a certain pump power, the numerator of R_T–the true coincidence originated from photon pairs, are the same for the two kinds of detunings because of the broadband nature of SFWM in DSF. However, the denominators of R_T, which is the accidental coincidence C_a determined by the total counts in signal and idler bands, including photons via the nonlinear processes of SFWM, RS and SPM, depends on detunings. At a certain pump power, single counts originated from SFWM are the same for the two cases, while the single counts contributed by RS are lower for the case with smaller detunings. Therefore, if SPM induced photons are negligibly small, the accidental coincidence rate for detuning of 4.4 nm should be lower than that for detuning of 5.6 nm. This is why TAR obtained with detuning of 4.4 nm is higher in the range of lower pump power levels. However, with the increase of pump power, the accidental coincidence for detuning of 4.4 nm grows faster than that for detuning of 5.6 nm, because SPM induced photons with smaller detuning increases more rapidly (see Fig. 4). Therefore, at high pump power levels, TAR obtained with the detuning of 4.4 nm become smaller than that with detuning of 5.6 nm, showing SPM induced photons are the noise background of photon pairs.

To further illustrate that the SPM induced photons are the background noise of photon pairs, we plot true coincidence rate as a function of the single count rate in idler band N_t', as shown in the inset of Fig. 6. One sees that there is no much difference between the data obtained with different detunings for N_t' in the low rate region. However, the true coincidence rate obtained with detuning of 4.4 nm is smaller for N_t' in the high rate region, within which the portion of SPM induced photons is higher for the data obtained with a smaller detuning. This is because SPM induced photons in signal and idler bands are not created in pair, thus, does not contribute to the true coincidence rate.

In conclusion, using 300 m DSF pumped by a pulsed pump with central wavelength in the anomalous dispersion regime of DSF, we have not only studied the influence of the SPM induced photons by measuring its dependence upon the detuning, upon the bandwidth and average power of pump pulses, but also clearly demonstrated that photon pairs via SFWM can be contaminated by the SPM induced noise photons.

Generally speaking, to develop an all fiber source of photon pairs in the telecom band with high quality, the side effect of SPM can be eliminated or mitigated by increasing the detuning, by decreasing the bandwidth of pump, or by exploiting a Sagnac fiber loop which has the ability to provide an extra 30 dB rejection to the spectrally broadened pump pulses [12, 20]. However,increasing detuning or decreasing the bandwidth of pump will result in the increased background noise via RS [2, 13]. Therefore, to improve the quality of the source of photon pairs, one need to balance the effects of RS and SPM by optimizing the source parameters, including the detuning and

the bandwidth of pump, so that the total noise photons produced by RS and SPM are maximally suppressed. Our detailed investigations of the influence of SPM is not only helpful for developing an all fiber source of photon pairs with low background noise in the telecom band, but also useful for exploring its applications.

Acknowledgement

This work was supported in part by the NSF of China (Grant No. 10774111, 11074186), the Specialized Research Fund for the Doctoral Program of Higher Education of China (Grant No. 20070056084), 111 Project (Grant No. B07014), and the State Key Development Program for Basic Research of China (Grant No. 2010CB923101).

References

[1] M. Fiorentino, P. L. Voss, J. E. Sharping, P. Kumar, Photon. Technol. Lett. 14 (2002) 983–985.

[2] J. G. Rarity, J. Fulconis, J. Duligall, W. J. Wadsworth, P. S. J. Russell, Opt. Express 13 (2005) 534–544.

[3] J. Fan, A. Dogariu, L. J. Wang, Opt. Lett. 30 (2005) 1530–1532.

[4] H. C. Lim, D. Wang, T. Tanemura, K. Katoh, K. Kikuchi, arXiv:quant-ph/0607179 (2006).

[5] O. Cohen, J. S. Lundeen, B. J. Smith, G. Puentes, P. J. Mosley, I. A. Walmsley, Phys. Rev. Lett. 102 (2009) 123603.

[6] H. Takesue, K. Inoue, Phys. Rev. A 70 (2004) 031802(R).

[7] H. Takesue, K. Inoue, Phys. Rev. A 72 (2005) 041804.

[8] E. A. Goldschmidt, M. D. Eisaman, J. Fan, S. V. Polyakov, A. Migdall, Phys. Rev. A 78 (2008) 013844.

[9] A. R. McMillan, J. Fulconis, M. Halder, C. Xiong, J. G. Rarity, W. J. Wadsworth, Opt. Express 17 (2009) 6156–6165.

[10] X. Li, L. Yang, X. Ma, L. Cui, Z. Y. Ou, D. Yu, Phys. Rev. A 79 (2009) 033817.

[11] M. A. Hall, J. B. Altepeter, P. Kumar, Opt. Express 17 (2009) 14558–14566.

[12] X. Li, J. Chen, P. L. Voss, J. Sharping, P. Kumar, Opt. Express 12 (2004) 3737–3744.

[13] X. Li, P. L. Voss, J. Chen, K. F. Lee, P. Kumar, Opt. Express 13 (2005) 2236–2244.

[14] H. Takesue, K. Inoue, Opt. Express 13 (2005) 7832–7839.

[15] S. D. Dyer, M. J. Stevens, B. Baek, S. W. Nam, Opt. Express 16 (2008) 9966–9977.

[16] X. Li, C. Liang, K. F. Lee, J. Chen, P. L. Voss, P. Kumar, Phys. Rev. A 73 (2006) 052301.

[17] H. Takesue, Appl. Phys. Lett. 90 (2007) 204101.

[18] X. Li, X. Ma, L. Quan, L. Yang, L. Cui, X. Guo, J. Opt. Soc. Am. B 27 (2010) 1857–1865.

[19] G. P. Agrawal, Nonlinear fiber optics (3rd edition), Academic Press, San Diego, 2001.

[20] D. B. Mortimore, J. Lightwave Technol. 6 (1988) 1217–1224.

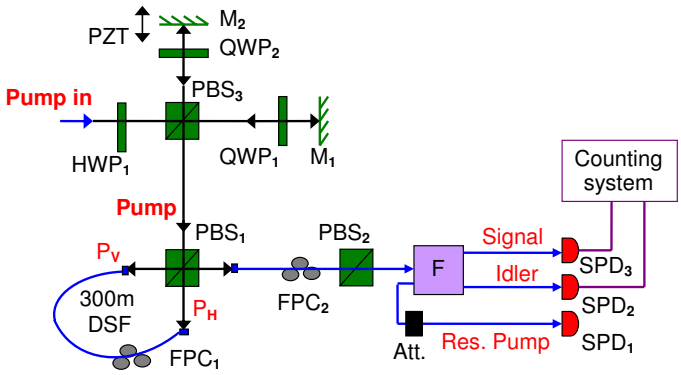

Figure 1: (Color online) A schematic of the experimental setup. PBS: polarization beam splitter; QWP: quarter-wave plate; HWP: half-wave plate; M: mirror; PZT: piezoelectric-transducer; FPC: fiber polarization controller; F: filter; Att.: attenuator; SPD: single photon detector.

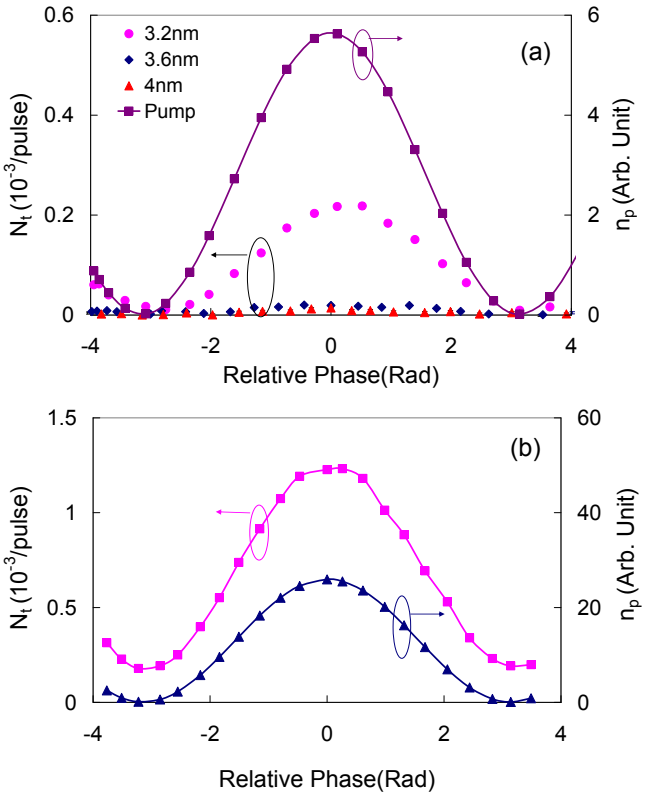

Figure 2: (Color online) Measured counting rate of the idler photons and attenuated pump photons, N_t and n_p, as a function of relative phase ϕ (a) when DSF is taken out, and the detuning is 3.2, 3.6 and 4 nm, respectively; and (b) when DSF is put back, and the detuning is 4 nm.

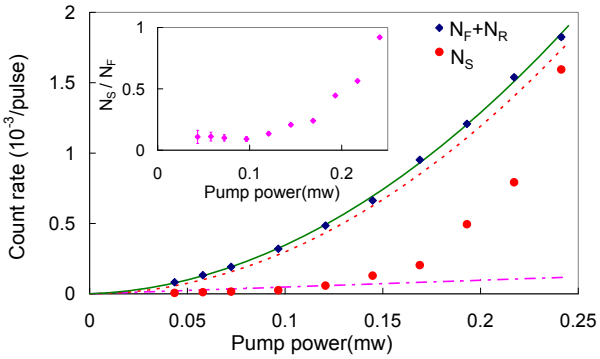

Figure 3: (Color online) The deduced counting rate of photons produced by SPM, N_S, and the sum of SFWM and RS, $N_F + N_R$, respectively, as a function of the average power of pump P_H (P_V). A second-order polynomial $N_R + N_F = s_1 P_{ave} + s_2 P_{ave}^2$ is used to fit the deduced data, and the contributions of linear scattering $N_R = s_1 P_{ave}$(dash-dot line) and quadratic scattering $N_F = s_2 P_{ave}^2$ (dot line) are plotted separately. The inset is the ratio N_S/N_F, as a function of the average power of P_H (P_V). The measurement is done at the detuning 4.4 nm.

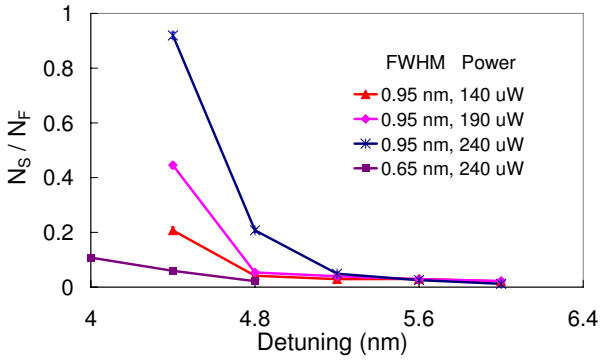

Figure 4: (Color online) The ratio of photons originated from SPM and SFWM, N_S/N_F, as a function of the detuning for the pump with different power levels and with different bandwidths. The solid lines are only for guiding eyes.

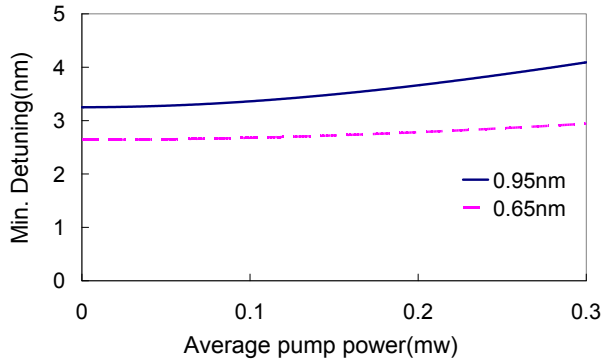

Figure 5: (Color online) Calculated minimum detuning of signal and idler photon pairs versus the average power of pump pulses with different FWHM.

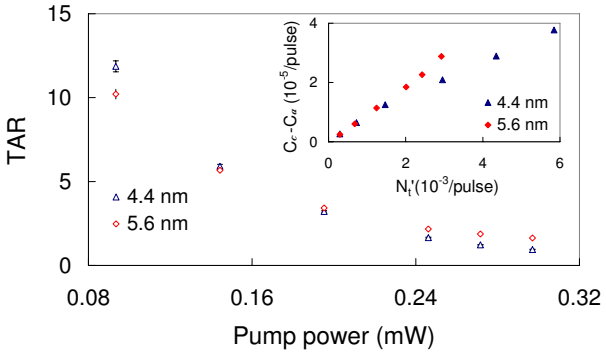

Figure 6: (Color online) The true-coincidence to accidental-coincidence ratio (TAR) of photon pairs versus pump power for detuning of 4.4 nm and 5.6 nm, respectively. The inset shows true coincidence rate $C_c - C_a$ as a function of the single count rate in idler band N_t'.